CSABA BURGER

PÉTER SZABÓ

RITA PONGRÁCZ

THE HUMAN FACTOR IN WILDFIRES:

TOWARDS A LONG-TERM FIRE RISK

ESTIMATION MODEL FOR CENTRAL BANKING

MNB WORKING PAPERS | 2

2026

THE HUMAN FACTOR IN WILDFIRES:

TOWARDS A LONG-TERM FIRE RISK ESTIMATION MODEL FOR CENTRAL BANKING

MNB WORKING PAPERS | 2

2026

MNB Working Papers 2026/2

The Human Factor in Wildfires: Towards a Long-Term Fire Risk Estimation Model for Central Banking

(Az emberi tényező a tűzmodellezésben: egy hosszú távú tűzkockázati modellezési megközelítés a központi bankok számára)

Written by by **Csaba Burger** (https://orcid.org/0009-0003-9566-6410), **Péter Szabó** (https://orcid.org/0000-0002-5921-5036), and **Rita Pongrácz** (https://orcid.org/0000-0001-7591-7989)

Budapest, 1st June 2026

Published by the Magyar Nemzeti Bank

Publisher in charge: Eszter Hergár

H-1013 Budapest, Krisztina körút 55.

www.mnb.hu

ISSN 1585-5600 (online)

Acknowledgements
The authors would like to thank Dr Imelda Somodi for her remarks on the MNB Working Paper. We also express gratitude to Dr. Bence Szabó for the discussion on good and bad controls. However, only the authors should be held responsible for errors, omissions, or opinions.

Contents

Abstract

Climate change elevated the relevance of fire risk projections for the future, which are essential for estimating the potential changes to expected economic losses, including the changing risk exposure of banking assets and insurance policies. And while the use of empirical models is required to lend credibility to this undertaking, human-induced fires, particularly stubble (or crop residue) fires, distort the observed relationship between weather and fire risk.

This paper presents an empirical–statistical model to estimate future fire risk using MODIS satellite data for fire occurrences, the Keetch-Byram Drought Index (KBDI) as weather-based input, and CORINE Land Cover information. The model is developed for Hungary at a 5 km resolution over the period 2001-2024. In addition, we account for the Human Factor (HF) in fire risk by introducing a Google Trends–based proxy reflecting legislation and public awareness of fire. Alternative definitions of this variable are also tested.

Incorporating the HF mitigates omitted variable bias, improves the explanation of past fire occurrences, and reverses the overall KBDI-fire risk relationship to the expected positive sign. Under the pessimistic RCP8.5 scenario, current fire occurrence risk is projected to double by the end of the century, with a potential of reaching a fivefold increase in extreme years, assuming the present HF in fire prevention and land cover flammability remain constant.

Journal of Economic Literature (JEL) codes: G21, G22, Q10, Q54
Keywords: climate change, fire risk, central banking, KBDI, causal graphs

Kivonat

A klímaválság fokozódásával a jövőre vonatkozó tűzkockázati előrejelzések egyre relevánsabbá válnak, és elengedhetetlenek a várható gazdasági veszteségek potenciális változásainak becsléséhez, beleértve a banki eszközök kockázati kitettségét. És habár empirikus modellek használata szükséges ennek meghatározásához, az ember okozta tüzek, különösen a tarlótüzek (vagy növényi maradványok), torzítják a megfigyelt kapcsolatot az időjárás és a tűzkockázat között.

Ez a tanulmány egy empirikus-statisztikai modellt mutat be a jövőbeli tűzkockázat becslésére. Ehhez a MODIS műholdas adatokat használtunk a tűzesetek beazonosítására, a Keetch-Byram aszályindexet (KBDI) időjárás-alapú magyarázóváltozóként, valamint CORINE felszínborítási információkat az éghető anyag közelítésére. A modellt Magyarország területére fejlesztettük 5 km x 5 km-es felbontásban, a 2001-2024 közötti időszak adatait felhasználva. Végezetül, a tűzkockázat emberi tényezőjét (Humán Factor, HF) egy Google Trends-alapú mutató bevezetésével képezzük le, amely a jogszabályokat és a közvélemény tűzzel kapcsolatos tudatosságát hivatott összefoglalni. E változó alternatív definícióit is teszteljük.

A HF beépítése mérsékli a becslés kihagyott változó miatti torzítottságát, javítja a múltbeli tűzesetek magyarázatát és a KBDI-tűzkockázat közötti általános kapcsolatot a várt pozitív előjelűre fordítja. A pesszimista RCP8.5 forgatókönyv szerint a jelenlegi tűzesetek kockázata várhatóan 66%-kal nő az évszázad végére, és akár négyszeresére is nőhet a szélsőséges években, feltételezve, hogy a tűzmegelőzésben és a földborítás gyúlékonyságában a jelenlegi HF állandó marad.

1 Introduction

One of the most severe consequences of climate change is the intensification of drought conditions, which in turn leads to elevated levels of wildfire risk. While existing methodologies for short-term fire risk estimation provide reasonably robust predictions over a horizon of several weeks, approaches for long-term fire risk assessment remain significantly underdeveloped. Yet, such long-term estimations are essential for evaluating decisions with far-reaching implications, particularly credit-related decisions, where accurate assessments of physical climate risks can materially influence outcomes. For financing institutions, and central banks in particular, addressing this gap is of critical importance.

Empirical evidence underscores the financial sector's growing sensitivity to physical climate risks. For instance, Euro-area banks with at least "adequate" levels of climate risk awareness in their lending practices charge, on average, an additional 4.4 basis points (BPs) in regions with "average" levels of physical risk, as opposed to no risk regions (Fontana et al., 2025). Similarly, Barbaglia et al. (2023) found that in Western Europe, banks charge an average premium of 6 BPs on loans to small firms located in high flood-risk areas. However, to the best of our knowledge, no publicly available study has yet examined whether such adjustments in lending rates are commensurate with the actual magnitude of underlying physical climate risks, wildfire or other.

One recent attempt to quantify the expected development of wildfire risk was undertaken by the European System of Central Banks' Expert Group on Climate Change and Statistics (Burger et al., 2024). This draft study estimates wildfire occurrence risk across Europe using extreme gradient boosting (xgboost), a statistical learning technique. However, the approach has several limitations. First, as a decision tree-based method, it predicts constant values for observations outside the range of its training data, resulting in static predictions for extreme climatic conditions not represented in the historical record. Second, and more critically, it deals with human-induced fires (up to 96% of all wildfires may be so, Dijkstra et al., 2022) with a technical tweak: the model is restricted to assume that higher weather-related fire danger always leads to higher wildfire risk through monotonicity constraints. While this adjustment aligns the model with physical expectations, its historical accuracy is limited, and does not contribute to the causal understanding of underlying processes.

Our paper estimates the long-term development of wildfire risk under multiple climate change scenarios, using Hungary as a case study. We incorporate both weather- and fuel-related determinants of wildfire occurrence (McNorton and Di Giuseppe, 2024), employing the Keetch–Byram Drought Index (KBDI; Keetch and Byram, 1968) as a key indicator of weather-related fire danger. Our data sources include MODIS satellite observations of historical fires, CORINE Land Cover raster maps, and daily KBDI values derived from HUCLIM gridded meteorological observations. The geographical focus is Hungary, covering the period 2001–2024 at a spatial resolution of 0.05° × 0.05°. Using these data, we project wildfire risk to the end of the 21st century under three divergent climate change pathways, RCP2.6, RCP 4.5, and RCP 8.5, and assess the implications of these projections for exposures within the Hungarian credit collateral portfolio.

A major contribution of this study lies in how we represent human-induced fires within statistical modelling. We propose a set of alternative variables to capture the Human Factor (HF), a proxy that integrates the combined effects of legislation, law enforcement, public awareness, and firefighting capacity. Among the indicators tested, we find that a Google Trends–based variable (constructed as the average relative popularity of climate, drought, and fire-related searches) offers the strongest contribution to explaining variations in wildfire occurrence risk. While previous studies have attempted to capture aspects of the human factor (e.g., Martínez et al., 2009), they generally fail to account for temporal variations and shifts in public behaviour.

Our results indicate that average wildfire occurrence risk is projected to increase by approximately 98% by the last quarter of the 21st century under the RCP 8.5 scenario, with risk levels nearly five times in extreme years, compared to today. These findings provide a foundation for defining theoretically informed credit risk mark-ups to account for climate change–induced wildfire risks.

The paper is structured as follows: Section 2 reviews the relevant literature and presents a causal framework for the regression analysis. Section 3 details the data, including the HF variable and the legislative context of fire protection, along with the applied methodology. Section 4 describes the statistical model development, and Section 5 presents projections of wildfire risk under various climate change scenarios. Section 6 concludes.

2 Literature

2.1 THE KEETCH-BYRAM DROUGHT INDEX (KBDI) EXPLAINING FIRE RISK

Weather-based fire danger indicators capture different temporal, meteorological, and fuel-related aspects of wildfire risk (Table 1), leading to varying predictive performance across vegetation types and precipitation regimes. We briefly discuss them to highlight our arguments for choosing the KBDI as the main driver for our fire risk estimations.

Table 1
Overview of the best-known fire risk index systems

	Fire weather index (FWI)	McArthur's Forest Fire Danger Index (FFDI)	National Fire Danger Rating System (NFDRS)
Described by	Wagner (1987)	McArthur (1967)	National Fire Danger Rating System (2006)
Direct weather patterns	Precipitation, humidity, temperature, wind speed	Wind speed, temperature, humidity	Wind speed, temperature, humidity
Fuel flammability	Fuel moisture codes	Drought factor (KBDI or SDI)	Fuel moisture models (Jolly et al. 2024)
Geographic focus	Developed for boreal forests but adapted globally	Australian eucalypt forests	Diverse US ecosystems

The Fire Weather Index (FWI) is a complex indicator designed to assess both fire ignition risk and potential fire spread (Wagner, 1987). It integrates temperature, rainfall, humidity, and wind speed into three moisture-related metrics: Fine Fuel Moisture Code (surface fuel dryness), Duff Moisture Code (medium-depth organic layer dryness), and Drought Code (deep soil moisture), and three fire behavior metrics: Initial Spread Index (ease and speed of ignition spread), Buildup Index (fuel availability and intensity), and the main output as Fire Weather Index. FWI reflects short-term weather conditions (typically one to two days) and is therefore responsive to rapid changes. The index ranges from 0 to 100, with values above 38 classified as "very high" and above 50 as "extreme" by the European Forest Fire Information System (Copernicus, 2019).

The McArthur's Forest Fire Danger Index (FFDI), commonly used in Australia, also incorporates weather and fuel moisture variables to estimate fire danger (Matthews, 2009). A key component of the FFDI is the Keetch–Byram Drought Index (KBDI), which estimates the amount of precipitation required to fully saturate the soil. KBDI is calculated using daily precipitation, maximum temperature (as evapotranspiration), and the previous day's KBDI value, thus reflecting cumulative soil moisture deficits over weeks and months. Unlike FWI, which is highly sensitive to short-term weather fluctuations, KBDI responds more gradually and is particularly effective at capturing persistent drought conditions. It is a valuable tool for modelling long-term fire danger, though less sensitive to short-term factors such as rainfall events or windspeed changes (Dowdy et al., 2009).

There are further differences between the drought-related components of the FFDI and FWI. While the Drought Code (DC) within the FWI captures deep organic moisture content at a depth of 10–20 cm, providing insights into the potential for sustained fires (Wagner and Pickett, 1985), its relevance is highest in ecosystems such as boreal forests, where deep organic layers play a dominant role in fire behaviour. In contrast, the KBDI focuses on the upper 20 cm of the soil profile, which directly influences the moisture content of surface vegetation and its flammability. This makes KBDI particularly relevant for shrublands and grasslands, where surface fuels dominate. As a result, KBDI tends to correlate more strongly with fire ignition risk, whereas the DC provides greater insight into smouldering potential. For example, conditions characterised by high KBDI but low DC values indicate elevated ignition risk, while the reverse suggests relatively manageable surface fire risk. In other words, the FWI may underestimate fire risk in regions where surface fuel is predominant.

The U.S. National Fire Danger Rating System (NFDRS), established in 1988, was designed for a broader range of applications beyond fire risk estimation, including prescribed burning and fire suppression strategies. This is achieved by combining multiple sub-indices into discrete fire potential levels, including the KBDI, the Energy Release Component (for estimating fire intensity), and the Burning Index (for predicting flame length). The fuel moisture sub-model within the NFDRS was recently refined by Jolly et al. (2024), who developed a generalised approach applicable across diverse vegetation types, including live and dead fuels. Their work underscores that incorporating long-term drought information – captured by the KBDI – is essential for generating accurate fire danger predictions.

While Sirca et al. (2017) found the FWI to be one of the strongest predictors of fire occurrence among several indices (including KBDI), its performance is not consistent across various conditions. Conversely, Andrade and Bugalho (2023) reported that the KBDI performs better in predicting fire ignitions.

In summary, the literature suggests that there are nuanced differences between fire risk indices. We reach out for KBDI given its rather simpler calculation method, and Hungary's temperate continental climate, which is, with its short and moderately cold winters, unlike the boreal forests of Canada. We also argue that the relatively simpler structure of the KBDI lends itself to more robust long-term projections in climate models compared to the FWI, which justifies its use as the primary weather-based fire danger indicator in this study.

2.2 HUMAN-INDUCED FIRES

A major challenge in modelling wildfire risk is determining whether and how to incorporate human-caused fires, intentional or unintentional. Dijkstra et al. (2022) report that an astonishing 96% of all wildfires are human-caused, including accidents, negligence and deliberate ignitions, despite the fact that up to half of fire events are officially recorded as having an unknown cause (de Rigo et al., 2017). Notably, Dijkstra et al. also find that the proportion of human-caused fires shows surprisingly low variability between countries and almost always exceeds 90%.

The Human Factor (HF) in wildfire occurrence risk is inherently multifaceted. One important driver is the presence of wildland–urban interfaces, which increase ignition likelihood (Leone et al., 2009). Conversely, depopulated or abandoned regions also elevate fire risk through the unsupervised accumulation of combustible materials (Pausas & Muñoz, 2012). Several studies have attempted to operationalise these dynamics. For example, Martínez et al. (2009) developed a model distinguishing human-caused from natural wildfire risks using predictors such as population change, land use transitions, infrastructure density, and patch-size metrics. Similarly, Padilla and Vega-García (2011) incorporated variables such as distances to towns and roads, land ownership categories (public, private, communal or protected). Prestemon and Butry (2010) applied Poisson autoregressive models to identify serial ignition patterns, treating repeated events similarly to recurring criminal activity.

Importantly, a model projecting future wildfire risk should not need to exclude all human-caused fires. For instance, power line ignitions are likely to remain relevant in the future, and such events should be retained in the data. By contrast, stubble burning, the deliberate burning of crop residues, represents a widespread but declining agricultural practice. While stubble burning has been banned in the European Union, the timing and enforcement of these bans vary considerably across member states. For example, in Portugal, the Institute for Nature Conservation and Forests reported that as of 2018, 66% of all recorded fires were still attributable to stubble burning (INCF, 2025).

Several studies have proposed methods for identifying and excluding stubble fires, but none are fully satisfactory for long-term projections. Demirdogen (2024) linked stubble fires to specific agricultural contexts, such as their higher incidence on corn fields and lower likelihood on land with livestock, cotton or forest cover. Xu and You (2023) approximated stubble fires by multiplying cropland share within a grid cell by fire size, assuming uniform fire distribution across land cover types, and it fails to capture sub-grid heterogeneity. The authors observed stubble fires around harvest times, but they also captured fires between harvests, which may not be stubble fires.

Other attempts involve focusing on lower-brightness fires detected by MODIS or VIIRS satellites or restricting analyses to daytime fires, under the assumption that farmers ignite fields during working hours (Liu et al., 2019; Coskuner, 2022). However, none of these approaches can reliably isolate human-induced fires, leaving models vulnerable to omitted

variable bias. This bias distorts parameter estimates, ultimately reducing the validity of both model coefficients and predicted fire occurrence risks.

To address this, we adopt a macro-level approach to incorporating HF. It is infeasible to disentangle the individual effects of legislation (e.g., various fire prevention laws introduced between 2001 and 2024), enforcement practices, public engagement, and climate-conscious vegetation management efforts (de Rigo et al., 2017). Instead, we propose the use of a single HF variable that aggregates these influences into one proxy measure. While it may be difficult to construct a fully causal quantitative model of the HF, a well-designed proxy can still significantly enhance predictive accuracy. The precise definition and operationalisation of this variable are provided in Section 3 (Data). For now, we assert the core tenet of this paper: a valid HF variable contributes meaningfully to improving wildfire occurrence predictions.

2.3 THE CAUSAL GRAPH EXPLAINING FIRE OCCURRENCE RISK

Fire danger indices are expected to exhibit varying relationships with wildfire occurrence depending on the land cover type. Since KBDI was originally developed to quantify fire ignition risk in Australian grasslands, its behaviour may differ in forest ecosystems. Accordingly, Burger et al. (2024) reported that higher forest cover was historically associated with lower wildfire occurrence, holding the fire weather index values constant. Such relationships are not constant, however: Cerasoli et al. (2016) observed increasing degradation of European eucalypt forests, while McDowell and Allen (2015) outlined how drought stress makes forests more susceptible to insect infestations, which in turn lead to greater accumulation of dead biomass and to increasing fire risk. All these imply in short that higher KBDI values are likely to imply a stronger increase in wildfire risk within forests than in other vegetation types.

Conversely, in agricultural areas, the relationship between KBDI and fire occurrence can be counterintuitive. High KBDI values may coincide with lower fire occurrence where fire bans constrain stubble burning practices. In addition, stubble burning typically occurs when crop residues are present, and conditions are too cold or humid for biological decomposition (Yıldırım, 2023). This implies a complex interplay between agricultural practices, legislation and weather conditions.

Recent policy and economic developments further complicate these dynamics. Net-zero initiatives and the growth of large-scale biomass energy production have provided alternative uses for crop residues. Since the late 2000s, biofuel production has emerged as a significant avenue for stubble utilisation (Herr et al., 2012). More recently, energy production from biomass (e.g. crop residues) has become a viable investment option for green enterprises in Hungary (Várgedő et al., 2025). All these suggest a rather complex, multi-way link between HF, croplands and fire risk.

Figure 1 summarises the expected relationships:

– Relationship A: Between HF and KBDI, indicating that people generally avoid starting fires in drier conditions, influenced by fire bans and risk awareness.

– Relationship B: Between HF and croplands, capturing how stubble burning practices are shaped by legislation (e.g. burning bans) and alternative uses (e.g. biofuels).

– Relationship C: Between KBDI and forests, reflecting the increased susceptibility of forests to ignition under dry conditions.

– Relationship D: A three-way interaction between HF, KBDI and croplands, suggesting that stubble fire use depends jointly on drought conditions and human/legal context.

– Relationship E: Between KBDI and croplands, for which no strong theoretical underpinning has been found (represented as a dashed line).

In summary, fire occurrence risk emerges from a complex network of interactions between weather conditions, land cover and HF. The following sections operationalise this framework and empirically test it.

Figure 1
The causal graph of hypotheses explaining fire occurrence risk

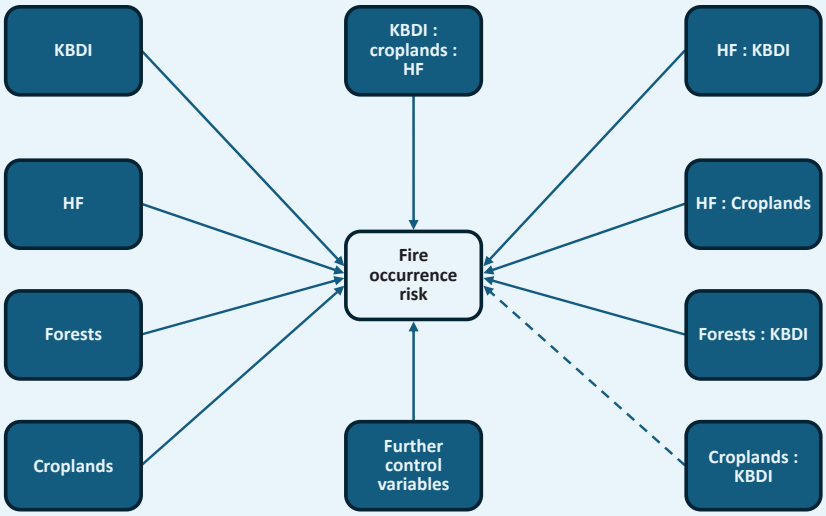

3 Data, Context and methodology

3.1 DATA

3.1.1 MODIS active fire monitoring

Vegetation fire data were obtained from the Moderate Resolution Imaging Spectroradiometer (MODIS), as provided by the NASA VIIRS Land Science Team (2021). Specifically, we used the combined Terra and Aqua MCD14 active fire product, derived from MODIS channels 21/22. This dataset provides fire detections at a 1 km² spatial resolution, with observations twice daily, and covers the period 2001-2024.

We restricted our analysis to presumed vegetation fires. Fire pixels in the raster files are detected based on the brightness temperature difference between the fire pixel and its background window, corrected for pixel size and scan angle, and scaled using coefficients that account for the spectral response of the 4 µm channel (Giglio et al., 2018). We did not apply additional filtering of fire pixels beyond these standard product adjustments.

3.1.2 Historical and projected KBDI values

For the historical period (2001–2024), we used the annually updated HUCLIM dataset, a high-quality, station-based, gridded observational dataset covering Hungary. HUCLIM provides daily homogenised meteorological variables, including precipitation and maximum temperature, at a 0.1° spatial resolution (Szentimrey, 2017). These data were obtained from HungaroMet (https://odp.met.hu) and served as input for computing historical KBDI values.

For future projections, we used outputs from Regional Climate Models (RCMs), which provide finer-resolution information on future climate conditions through dynamical downscaling of Global Climate Models (GCMs). We evaluated three Representative Concentration Pathways (RCPs) (Van Vuuren et al., 2011): RCP2.6, consistent with limiting warming to 2 °C in line with the Paris Agreement; RCP4.5, a stabilisation pathway with reduced emissions post-2040; and RCP8.5, a high-emissions "business-as-usual" scenario with minimal mitigation.

For each RCP, we used six RCM-GCM simulations at 0.125° spatial resolution, provided by the EURO-CORDEX initiative (Kotlarski et al., 2014; Jacob et al., 2014). These combinations are summarised in Table 2, which also indicates that all RCM–GCM pairs were simulated under each scenario, including historical runs.

Table 2
RCM–GCM pairs used in the analysis. In addition to the historical simulations, each pair was used under all three RCP scenarios.

↓RCM\GCM →	CNRM-CM5	EC-EARTH	NorESM1-M
ALADIN63	X		
CCLM4-8-17		X	
HIRHAM5		X	
RACMO22E	X		
RCA4			X
REMO2015			X

To focus on the period of highest wildfire risk, we restricted both historical and projected datasets to the June-September (JJAS) season, representing the driest soils and hottest months of the year, and as such, we calculated the mean KBDI value for the months of JJAS. Although daily maximum values over a month are historically accurate and contain additional information from a fire risk standpoint, their robustness in future projections is lower compared to their monthly mean values.

To correct inherent model biases, we applied a distribution-based bias correction directly to the monthly mean KBDI values of each model, rather than correcting the individual input climate variables separately, then took their mean over JJAS. This approach preserves the physical consistency between variables. The monthly bias correction was performed using standardisation, aligning the modelled values (MOD) with HUCLIM observations (OBS) for the baseline period (2001–2024):

$$\mathrm{CORR_t} = \frac{\mathrm{MOD_t} - \mathrm{MOD_{mean\_2001-2024}}}{\mathrm{MOD_{var\_2001-2024}}} \cdot \mathrm{OBS_{var\_2001-2024}} + \mathrm{OBS_{mean\_2001-2024}}$$

where t denotes individual years, mean and var are means and standard deviations for the respective datasets. This method adjusts both the monthly mean and variability of the simulated values to match the observational distribution in the past.

To minimize uncertainties associated with individual model selection, we used the mean across the six RCM–GCM combinations within each grid cell and year. This ensemble approach provides robust central estimates and facilitates easier interpretation for stakeholders.

3.1.3 Proxy for the Human Factor variable

Capturing the combined effects of legislation, enforcement, public awareness, and actions related to wildfire prevention is inherently challenging and involves subjective choices. However, these elements tend to evolve together in response to the visible impacts of climate change and rising societal awareness of physical risks.

While comprehensive media-based analyses, such as those by Aoyagi et al. (2025) and Appelgren et al. (2025), could be incorporated using aggregated, annualised European time series, we opted for a more direct proxy based on Google Trends (GT) data for Hungarian-specific HF. GT provides normalised monthly search volumes (scaled 0-100) for selected terms, reflecting public interest in specific topics. We extracted GT data for “climate” (“klíma”), “drought” (“aszály”), and “fire” (“tűz”), summed them to annual values, and applied a two-year moving average to account for lagged behavioural responses to preceding-year droughts. As GT data are only available from 2004 onwards, we extended the earliest available value backwards to 2001-2003, assuming minimal change in public awareness during this period.

To test robustness, next to the above-mentioned terms, we also considered alternative HF-definitions:

- Atmospheric CO_2 concentrations (Mauna Loa, NOAA), capturing a physical but non-country-specific and multi-year driver of KBDI;
- European newspaper coverage of climate change (Appelgren et al., 2025), a uniform Europe-wide proxy of climate awareness;
- Annual GT metrics for “ozone” and “AI” (placebo tests with unrelated topics).

The absolute scale of the HF variable is irrelevant, and its role lies in capturing relative changes over time. Aggregated HF data are provided in Appendix 1.

3.1.4 Further data sources

The analysis incorporates CORINE Land Cover (CLC, 2018) data to represent land cover characteristics. Although the six-year re-measurement interval may limit applicability in rapidly changing regions, it provides sufficient temporal resolution for Hungary, where large-scale land cover changes are not frequent. Land cover categories were aggregated into artificial, agricultural, forest, wetland and water bodies, with additional subdivisions applied to agricultural and forest areas to balance classification details.

Elevation and slope data is from the EU Digital Elevation Model (EU DEM) (European Commission, 2012), which have been identified as significant determinants of wildfire risk in previous studies (Abdollahi and Pradhan, 2023). While these values were calculated for the centre of each grid cell, we also added their standard deviation measures within each cell to control for within-cell spatial variations.

To approximate potential economic exposure, real estate collateral data were sourced from the Hungarian National Credit Register (HITREG). This dataset contains information on 743,000 collaterals, representing a total market value of 36 trillion HUF (≈89 billion EUR) as of 2024, reported at postal code level. Given the absence of damage functions, only the spatial distribution of collaterals was considered, assuming uniform allocation within postal zones. This is an acceptable simplification for wildfire risk, compared with hazards requiring finer spatial precision, such as floods.

3.1.5 Spatial and temporal data aggregation

All datasets were converted to a 0.05° × 0.05° grid (approximately 5 km × 5 km), representing a balance between the coarser 0.1° resolution of KBDI values, the finer 0.01° resolution of MODIS fire detections, and the 100 m resolution of CORINE Land Cover data. Geographic elevation and slope values correspond to the cell center, while land cover variables represent the proportional coverage of each class within the grid cell.

The target variable, a binary fire flag, was set to 1 if at least one fire event was recorded within a grid cell during the JJAS season and 0 otherwise. KBDI values were averaged for the JJAS months, while further variables are constant for a year or more, hence, these did not require aggregation.

3.2 CONTEXT

The data is relevant for this paper for the following reasons. Firstly, Hungary's temperate continental climate makes it particularly vulnerable to climate change, with rising drought frequency posing risks to both ecosystems and the economy. Agriculture dominates 56% of the country's land area, as seen visible from the land cover data, mostly crop fields.

Secondly, policy changes over the past two decades have substantially influenced wildfire dynamics. Hungary's EU accession brought the enforcement of a stubble burning ban in 2012, coinciding with a marked decline in fire occurrences (**Figure 2**). Key legislative milestones include the 2008 decree on forest fire protection (4/2008. (VIII.1.) ÖM), the 2009 Act on forest management and wildfire prevention (2009/XXXVII), and the 2011 disaster protection law (2011/CXXVIII). This latter law centralised firefighting under a national service, which had been funded and run locally before that. Later regulations significantly restricted open-field biodegradable waste burning (2012/CLXXXV) and introduced uniform national fire prevention rules (54/2014 (XII.5)). In 2017, the right to impose open fire bans were drawn from local authorities to the Ministry of Agriculture, and have since become a dynamic, spatially varying, regularly updated practice.

Figure 2
The development of monthly fire frequencies (number of 0.5 x 0.5 degrees grid cells with fire as a share of all grid cells). Note that this plot reflects values for all months, not just for the main fire season between June and September.

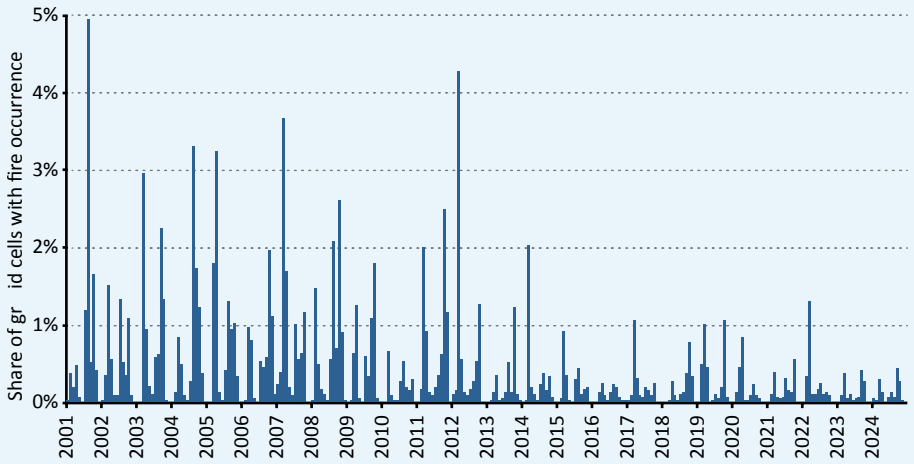

While these measures have contributed to reducing fire frequencies, their impact appears to have plateaued. Consequently, in projecting future wildfire risks, the HF variable is held constant at its recent observed level.

3.3 METHODOLOGY

Approaches to estimating wildfire occurrence risk range from logistic regressions to complex machine learning models such as neural networks (Abdollahi & Pradhan, 2023). Recent studies, including McNorton et al. (2024) and Burger et al. (2024), applied gradient boosting models to capture nonlinear interactions between predictors. In contrast, this study employs a logistic regression model for three reasons: (i) tree-based models fail to extrapolate beyond the range of training data, producing constant predictions for future KBDI values outside observed ranges; (ii) the regional scope of this study limits the number of observations and geographic heterogeneity, reducing the need for a very complex modelling; and (iii) logistic regression offers greater interpretability, since the former contains ex ante defined interactions only. As opposed to that, gradient boosting grows decision trees in a sequential manner, thereby it builds interactions by design, which are to be analyzed and studied in detail, if we want to uncover relationships.

Therefore, the baseline model is specified as follows:

$$Fire\ occurrence = \beta_0 + \beta_1 KBDI + \beta_2 HF + \beta_3 Elevation + \beta_4 Slope + \sum_i \beta_i LC_i$$

where 'Fire occurrence' is a binary variable indicating the presence (1) or absence (0) of a fire in a grid cell during the JJAS season; KBDI is the mean value for JJAS; HF represents the annual Human Factor; Elevation (m) and Slope (rad) describe topography at the grid cell center; LC_i denotes land cover shares. To avoid multicollinearity, heterogeneous agricultural activities (i.e. 'Annual crops associated with permanent crops', 'Complex cultivation patterns', 'Land principally occupied by agriculture, with significant areas of natural vegetation' and 'Agro-forestry areas'), wetlands and water bodies (covering 21% of Hungary) are excluded from the regression.

To test the hypotheses underlying the causal graph (**Figure 1**), interaction terms between KBDI, HF, and the shares of cropland and forest are introduced. Given that variable interactions complicate coefficient interpretation, partial dependency plots are used to present projected probabilities for average observations as predictors vary between their minimum and maximum values.

The estimated models are applied to project future fire occurrence risk using KBDI values from climate simulations, assuming constant regression parameters and land cover shares over time. While this enables scenario-based projections, it represents a key limitation of the study, as both vegetation flammability and land cover may evolve under changing climatic and socio-economic conditions.

4 Fire risk estimation

4.1 MODELLING FIRE OCCURRENCE RISK

Figure 3 shows the share of grid cells with recorded fires for all months (blue) and for JJAS (red), along with the five-year moving average of KBDI values averaged over the country. While fire frequency declined over time for both the full year and JJAS, KBDI values exhibited an upward trend, particularly during JJAS, suggesting that the relationship between KBDI and fire frequency is not straightforward.

Figure 3
Share of grid cells with at least one fire event

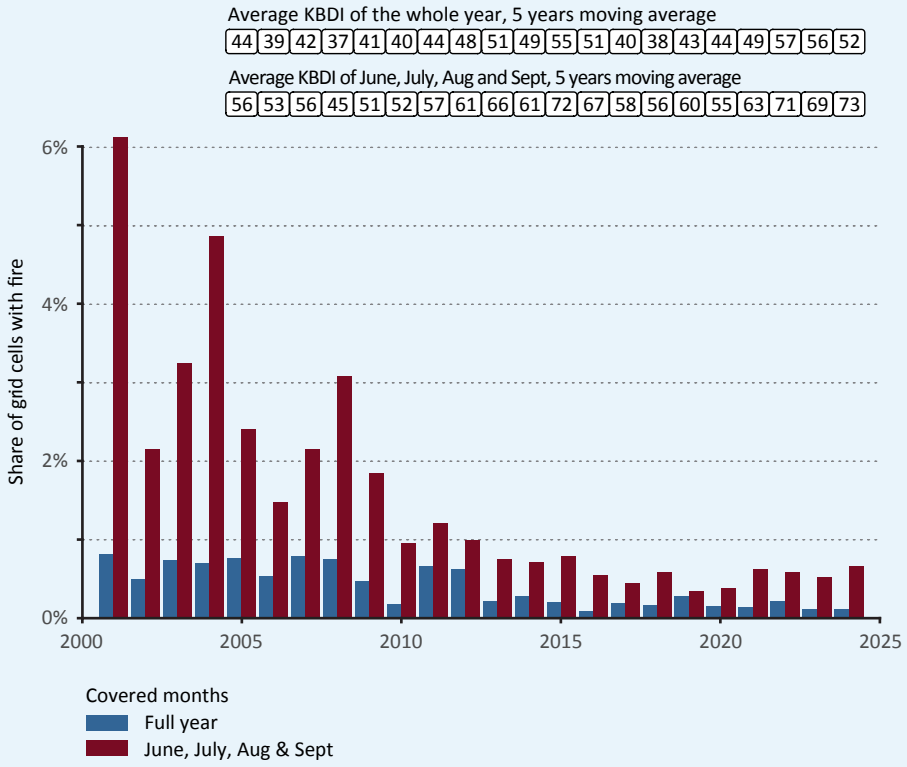

The relationship between KBDI and fire frequency is further explored in **Figure 4**, which stratifies fire frequencies by KBDI category, cropland share (above/below 40%), and before/after 2012 observations, for June-September (JJAS) only. Fire frequency decreased across all KBDI categories after 2012, regardless of cropland share. This pattern appears counterintuitive given the physical link between drought and fire risk, suggesting that institutional or behavioural factors, such as stubble burning bans, affect the relationship as well. Given that croplands cover over 50% of Hungary, ignoring this dynamic could distort the model.

Figure 4
Share of grid cells with fire by period and cropland share, JJAS only

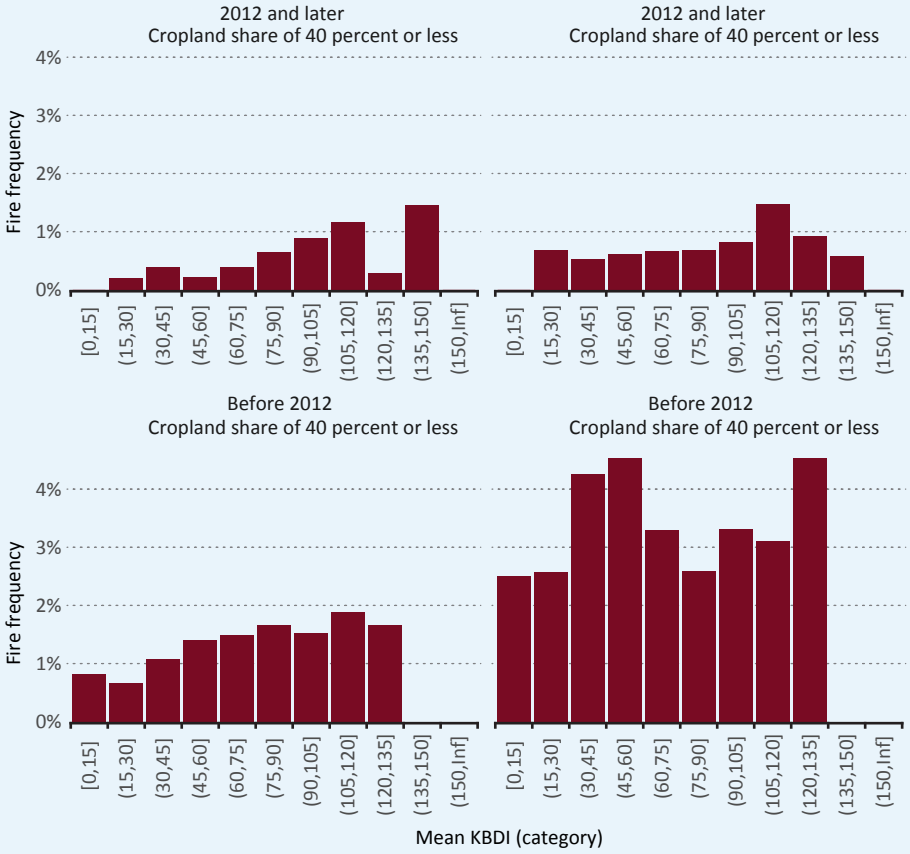

The absolute values of pairwise Pearson-correlations are in a few cases high and significant (**Figure 5**). Removing highly correlated predictors is not a strict requirement for statistical inference or unbiased predictions. It is necessary only if the individual coefficients of the independent variables are to be interpreted further, and/or are used for climatic projections.

With that in mind we suggest removing the share of forest land cover variable, given its high correlation with arable land cover share. By doing so, we will be unable to prove the suspected relationship between drought and fire frequency in forests. In addition, one elevation-related variable is sufficient to express variations in the data, hence, we suggest keeping elevation only. Note that the same conclusions would be drawn if we based our decisions on Spearman-correlation values.

Figure 5
Pairwise Pearson-correlations between the explanatory variables used for the analysis. The upper triangle shows correlation values, whereas the lower triangle contains stars corresponding to their significance levels (* = 0.1%, ** = 1%, * = 5%)**

	KBDI mean	Human Factor	Share of croplands	Share of permanent agriculture	Share of forests	Share of artifical land cover	Share of wetlands	Share of open water	Elevation	Slope	Elevation sd	Slope sd
KBDI mean		0,2***	0,16***	-0,01	-0,18***	-0,02***	0,02***	0,02***	-0,34***	-0,23***	-0,27***	-0,26***
Human Factor			-0,02***	-0,02***	0,02***	0,02***	0	0	0	0	0	0
Share of croplands				-0,19***	-0,76***	-0,16***	-0,15***	-0,18***	-0,46***	-0,38***	-0,45***	-0,44***
Share of permanent agriculture					-0,05***	0,04***	0,04***	-0,02***	0,01**	0,03***	0,1***	0,13***
Share of forests						-0,21***	-0,02***	-0,1***	0,56***	0,42***	0,46***	0,4***
Share of artifical land cover							-0,04***	0,06***	-0,01***	0	0,08***	0,1***
Share of wetlands								0,15***	-0,1***	-0,07***	-0,06***	-0,04***
Share of open water									-0,11***	-0,04***	0,01**	0,07***
Elevation										0,68***	0,77***	0,69***
Slope											0,61***	0,55***
Elevation sd												0,94***
Slope sd												

The logistic regression models (**Table 3**) use JJAS fire occurrence as the dependent variable. Regression 1 includes KBDI, land cover, and elevation, showing an unexpected negative sign for KBDI, likely due to omitted variable bias. Adding HF (Regression 2) reduces this bias, and the coefficient of KBDI moves close to zero. Regression 3 incorporates all interactions between KBDI, cropland, and HF. KBDI, HF, and cropland were centered to avoid multicollinearity in the interaction terms. Given that all Variance Inflation Factor (VIF) values stay below 5, multicollinearity does not distort the coefficients (highest VIF values are 1.5, 1.5 and 2.3 for Regressions 1,2 and 3 respectively).

Table 3
Logistic regressions explaining the log odds of a fire is present in a cell

	Dependent variable: Fire occurrence		
	Regression 1	**Regression 2**	**Regression 3**
KBDI mean (centered)	-0.005***	-0.001	0.006***
	(0.001)	(0.001)	(0.001)
Human Factor (centered)		-0.005***	-0.004***
		(0.0002)	(0.0002)
Arable agriculture land cover	1.711***	1.634***	0.904***
	(0.116)	(0.116)	(0.142)
Permanent agriculture land cover	-0.243	-0.811	-0.811
	(0.555)	(0.572)	(0.571)
Artificial land cover	-1.061***	-0.828**	-0.771**
	(0.379)	(0.373)	(0.369)
Wet land cover	2.255***	2.182***	2.191***
	(0.557)	(0.568)	(0.568)
Open water land cover	-3.521***	-3.627***	-3.548***
	(0.855)	(0.861)	(0.854)
Elevation	-0.003***	-0.003***	-0.002***
	(0.0005)	(0.0005)	(0.0005)
KBDI mean (centered) : Human Factor (centered)			0.00004***
			(0.00001)
KBDI mean (centered) : Arable agriculture land cover			-0.005
			(0.004)
Human Factor (centered) : Arable agriculture land cover			-0.006***
			(0.001)
KBDI mean (centered) : Human Factor (centered) : Arable agriculture land cover			0.00003
			(0.00002)
Max VIF value	1.5	1.5	2.3
Observations	117,936	117,936	117,936
Log Likelihood	-9,203.112	-8,767.740	-8,691.501
Akaike Inf. Crit.	18,422.220	17,553.480	17,409.000

*Note: (*p<0.1; **p<0.05; ***p<0.01)*

To assess overall model performance, we randomly split the data into 90% training and 10% testing sets, estimated each regression on the training data, and calculated AUROC (area under the receiver operating characteristic), precision, and recall values on the test sets. To reduce sensitivity to any single split, this process was repeated 100 times, with summary results reported in **Table 4**.

Table 4
Bootstrapped logistic regression performance metrics (on 100 randomly drawn 90% training / 10% testing sets, cutoff for precision and recall at mean fire frequency)

Model	AUROC mean	AUROC 95% CI	Precision mean	Precision 95% CI	Recall mean	Recall 95% CI
Regression 1	0.661	0.627-0.692	0.024	0.019-0.028	0.658	0.591-0.719
Regression 2	0.748	0.72-0.778	0.032	0.027-0.036	0.742	0.686-0.795
Regression 3	0.751	0.728-0.783	0.035	0.029-0.04	0.696	0.649-0.76

Model performance metrics show a marked improvement in AUROC and in precision between Regressions 1 and 2, and show minor and probably insignificant improvements between Regression 2 and 3. Recall values improve when we move from Regression 1 to 2, but falls slightly back at Regression 3. **Figure 6** puts the model performance into perspective: it displays average observed fire frequencies alongside predicted probabilities from Regression 1 (baseline without the Human Factor or interactions), Regression 2 (with Human Factor), and Regression 3 (full model). Regression 3 tracks observed values most closely, indicating the benefit of including interaction terms. We therefore choose to proceed with Regression 3 for future analyses.

Figure 6
Projected fire probabilities and observed frequencies, JJAS only

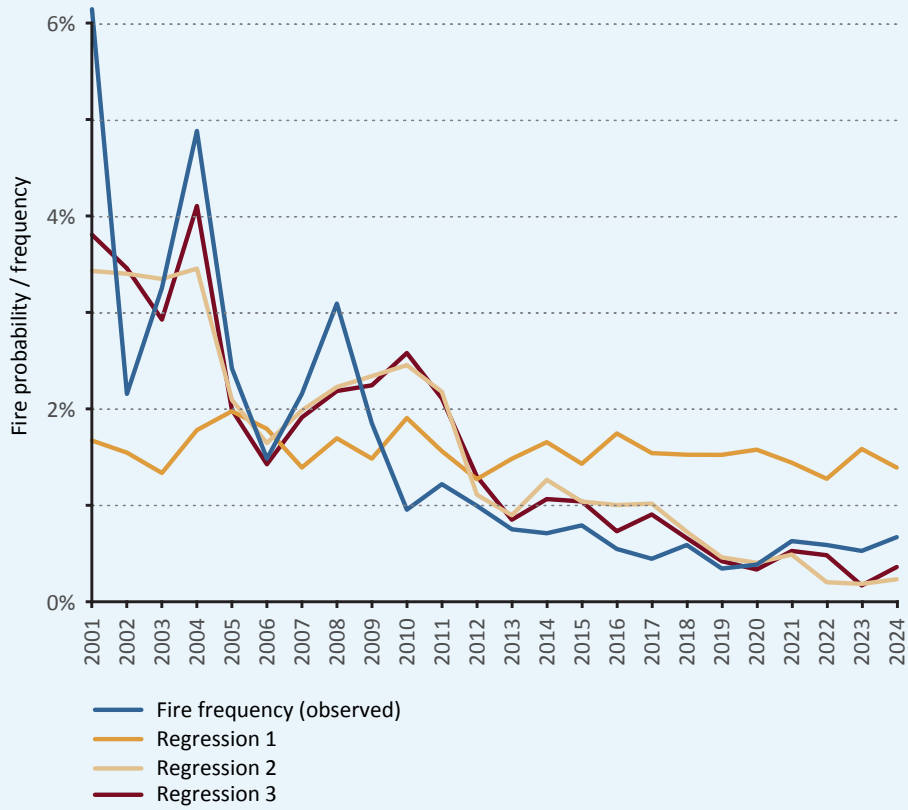

The full effect of the interaction terms in Regression 3 is investigated further with the help of partial dependency plots (or interaction plots), of **Figure 7**. These show the predicted fire probabilities when selected predictors are moved from their minimum to their maximum values, holding all other variables constant. **Figure 7/A** demonstrates a diminishing marginal effect of the HF, with the curve flattening as values increase. Moreover, at high KBDI levels (e.g., 150), the sensitivity of fire risk to changes in HF decreases. **Figure 7/B** incorporates human behaviour in the KBDI-fire probability relationship. At low HF values, typical in the first decade of the 2000s, the relationship between KBDI mean and fire probability is negative. While this may sound counterintuitive at first, the habit of starting stubble fires of campfires when drought was not present, which is avoided in arid conditions, may explain that. Before regulations, fires were more frequent at low KBDI, indicating likely human ignition. In recent years, such behaviour diminishes, and fire occurrence aligns more with environmental stress.

Finally, **Figure 7/C** shows that cropland land cover share reacts strongly to various Human Factor levels. At low HF values, fire risk is high. In addition, when HF is high, fire risk is higher, the lower the share of cropland is. In other words, when fire precautions are made, fire risk is higher with more non-cropland[1].

[1] When cropland share is reduced, another land cover type is increased to remain at 100 percent. I moved forest land cover share in the other direction. Since forest land cover is not directly modelled, we cannot say with certainty if the behaviour seen on the plots is driven by forests.

Figure 7
Partial dependency plots using Regression 3, showing predicted fire probabilities

Figure 7/A: Human factor variable

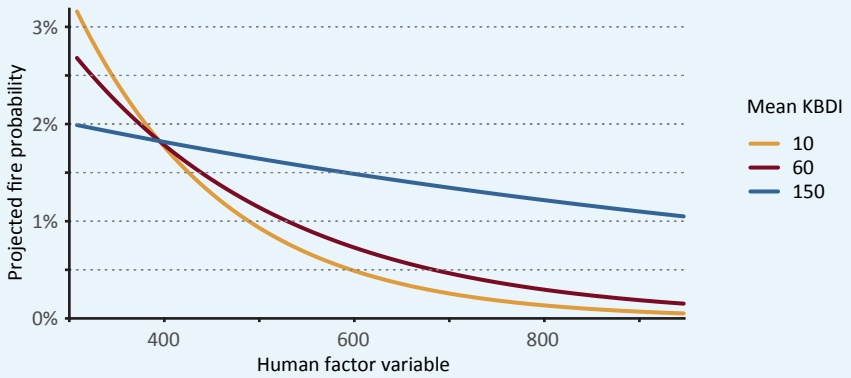

Figure 7/B: Impact of mean KBDI

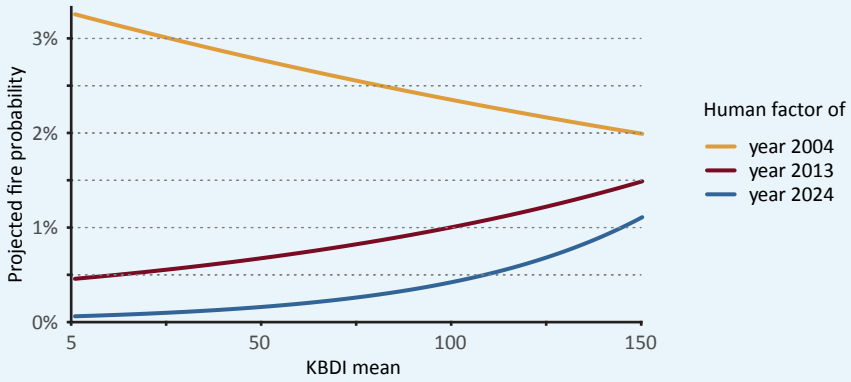

Figure 7/C: Impact of Human Factor and cropland land cover share on fire risk

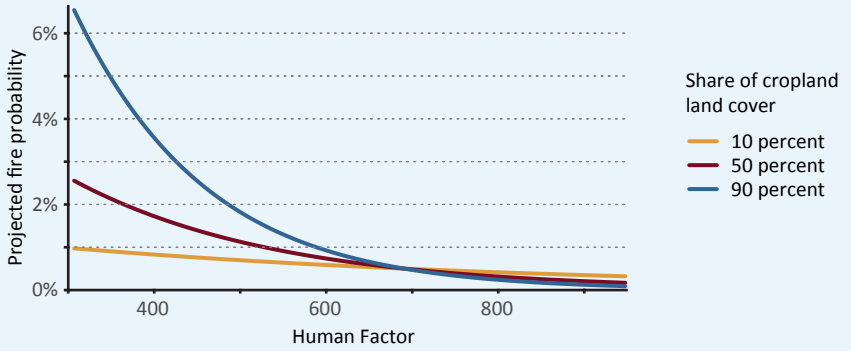

A final assessment of Regression 3, **Figure 8**, compares observed fire frequencies (bars) with predicted fire probabilities (lines) for the periods 2001-2004 and 2022-2024. While the overall level and trend of fire frequencies are well captured (noting the differing vertical scales), the model underestimates the high fire frequencies in the low-KBDI categories. Conversely, it correctly captures the exponential increase at high KBDI levels in recent years.

Figure 8
Average fire frequencies and projected probabilities for JJAS

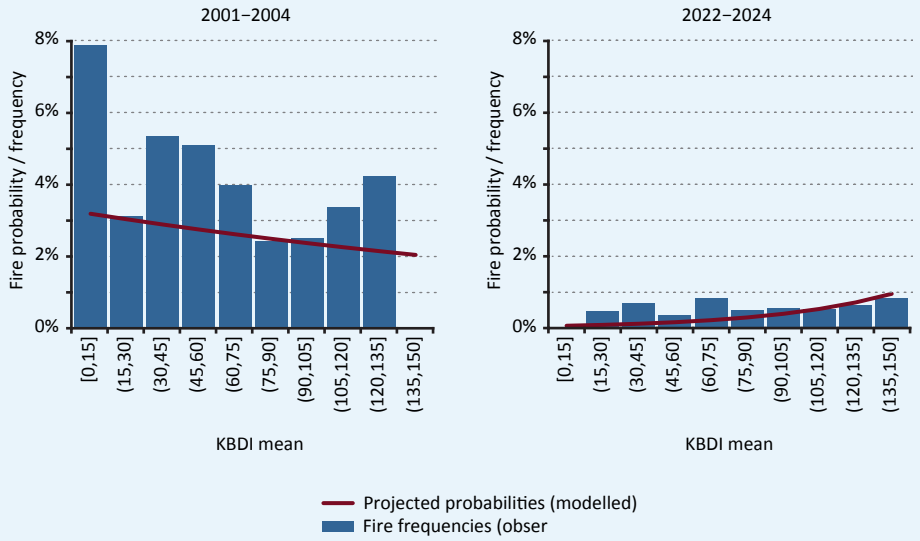

4.2 ALTERNATIVE HUMAN FACTOR DEFINITIONS

To test the robustness of the HF, we evaluated alternative definitions using both theoretically relevant and unrelated proxies (**Table 5**). Unrelated variables include GT search terms such as "COVID", "AI", and "bioethanol", while alternative climate-related proxies include the atmospheric CO_2 concentration and the volume of climate-related press publications in major European outlets (Appelgren et al., 2025). As expected, models using unrelated terms perform substantially worse. The CO_2-based time series has higher performance metrics than the original GT-based specification.

Table 5
Bootstrapped regression performance values using alternative Human Factor variable definitions (on 100 randomly drawn 90% train / 10% test split, cutoff for precision and recall at mean fire frequency)

Human Factor definition	AUROC mean	AUROC 95% CI	Precision mean	Precision 95% CI	Recall mean	Recall 95% CI
Google Terms term 'COVID'	0.705	0.67-0.733	0.026	0.022-0.031	0.713	0.651-0.778
Google Terms term 'bioethanol'	0.713	0.682-0.754	0.029	0.024-0.034	0.586	0.521-0.661
Google Terms term 'AI'	0.723	0.696-0.755	0.030	0.025-0.035	0.646	0.6-0.708
Press publications	0.727	0.691-0.763	0.031	0.026-0.037	0.609	0.538-0.681
Regression 3 (original HF def.)	0.751	0.728-0.783	0.035	0.029-0.04	0.696	0.649-0.76
Atmospheric CO_2-concentration	0.769	0.74-0.801	0.036	0.03-0.041	0.718	0.661-0.781

Although AUROC scores are similar across the best-performing HF definitions, the original GT-based version seems to track observed fire frequencies closer, particularly from 2013 onwards (**Figure 9**). This supports the use of the original GT-based HF as a valid and dynamic proxy.

Figure 9
Projected fire probabilities in Regression 3 using alternative Human Factor definitions

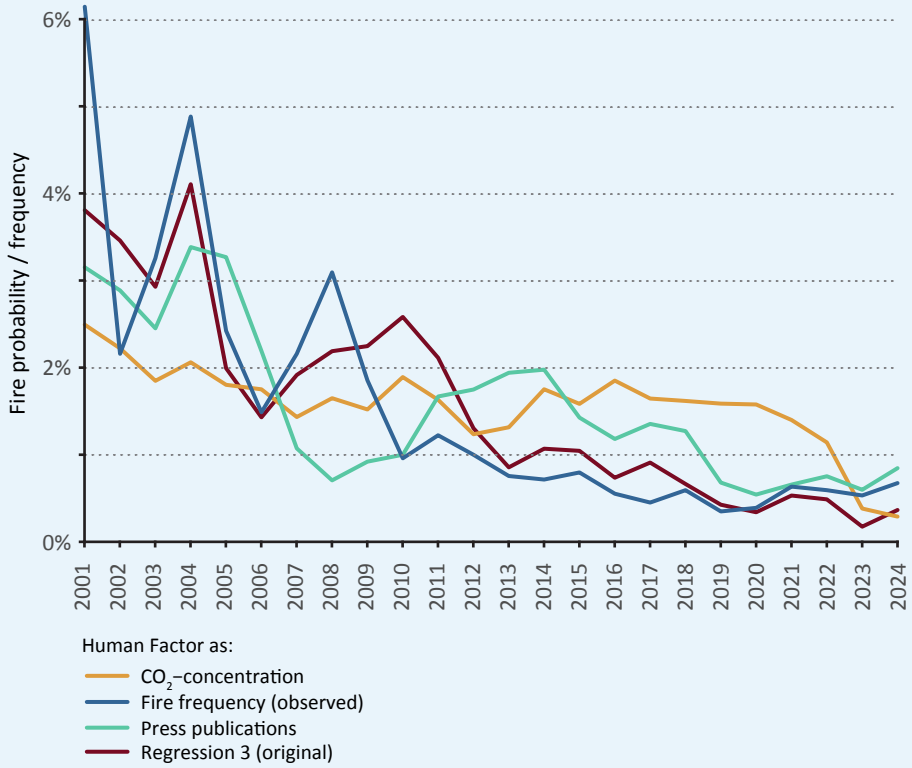

5 Future fire risk exposures

To assess the potential impacts of climate change on wildfire risk, we use KBDI simulations under three Representative Concentration Pathways (RCP2.6, RCP4.5 and RCP8.5), focusing on the June-September (JJAS) period. RCP8.5 features higher atmospheric CO_2 concentrations, accompanied by increased temperature and evapotranspiration potential, and its effect on fire-weather indices is straightforward. We are aware of that in the Mediterranean region elevated CO_2 levels are expected to increase fire danger (Carnicer et al., 2022). We hold the Human Factor constant at their latest, 2024 value when working with predictions, and we use this value for 'backcasting' fire risk for the 2001-2024 period.

Table 6 presents the projected monthly mean fire risk by period and scenario, for the mean (representing the average fire probability in the JJAS months per month within the period), the confidence intervals of the mean (stemming from the uncertainty of the statistical model presented above), and the 95th percentile of the various climatic projections (whereby a fire occurrence probability was estimated for all KBDI values appearing within each climatic model, and the 95th percentile of these values was determined), and the confidence interval of the 95th percentile (the statistical uncertainty of the extreme climatic value). This last value includes the (upper end of the) uncertainty coming from the various climatic models and the statistical estimation. Values are aggregated for the country.

Results indicate stagnating risk levels in the RCP2.6 scenario, with a slight increase in the 95th percentile values, only to be followed by a slight decline towards the end of the century. While RCP 2.6 will certainly not materialize, its values serve as a baseline which would have been possible for humanity. The mean values for the RCP4.5 and 8.5 move upwards already in the next 25 years. These scenarios start to differ meaningfully only towards the end of the century. Years with extreme fire danger are expected to produce summers with higher fire risk values in the 2025-2049 period already: the 95th percentile values reach for the RCP 4.5 and RCP 8.5 0.92 percent and 0.80 percent respectively.

The highest increase is to arrive in the RCP 8.5 towards the end of the century, whereby fire is expected in more than 1 percent of all grid cells in extreme years in JJAS months. To summarize: current fire risk is to increase by 95 percent (0.43% / 0.22%) by the end of the century in the RCP 8.5; with extreme years where fire risk is to grow five times to its current level (1.18% / 0.22%), which may be even higher (1.38% / 0.22%).

Table 6
Projected monthly average fire risk values (JJAS only) (a visualization to alleviate interpretations is in Appendix 3)

Period	KBDI values based on	Mean	CI (95%)	95th percentile of KBDI values within climate models	CI (95%) of the 95th percentile
2001-2024	ObservationsI	0.22%	NA	NA	NA
2025-2049	RCP 2.6	0.25%	0.16-0.35%	0.68%	0.58-0.77%
	RCP 4.5	0.32%	0.16-0.49%	0.92%	0.76-1.08%
	RCP 8.5	0.28%	0.16-0.39%	0.80%	0.69-0.91%
2050-2074	RCP 2.6	0.25%	0.15-0.35%	0.69%	0.59-0.79%
	RCP 4.5	0.31%	0.17-0.45%	0.86%	0.72-1%
	RCP 8.5	0.29%	0.17-0.42%	0.87%	0.74-1%
2075-2099	RCP 2.6	0.24%	0.15-0.33%	0.65%	0.56-0.74%
	RCP 4.5	0.31%	0.17-0.46%	0.89%	0.74-1.04%
	RCP 8.5	0.43%	0.23-0.63%	1.18%	0.98-1.38%

We assessed the geography of the projected fire risk metrics and their changes, using the means (expected values, **Figure 10**). Fire risk is expected to increase nationwide, with particularly notable high changes in the Great Plain's large agricultural areas, as well as in wetlands near Lake Balaton and around the Hortobágyi National Park near Debrecen.

Figure 10
JJAS monthly projected mean fire risk values for 2001-2024, for 2075-2099 and their changes following RCP8.5.

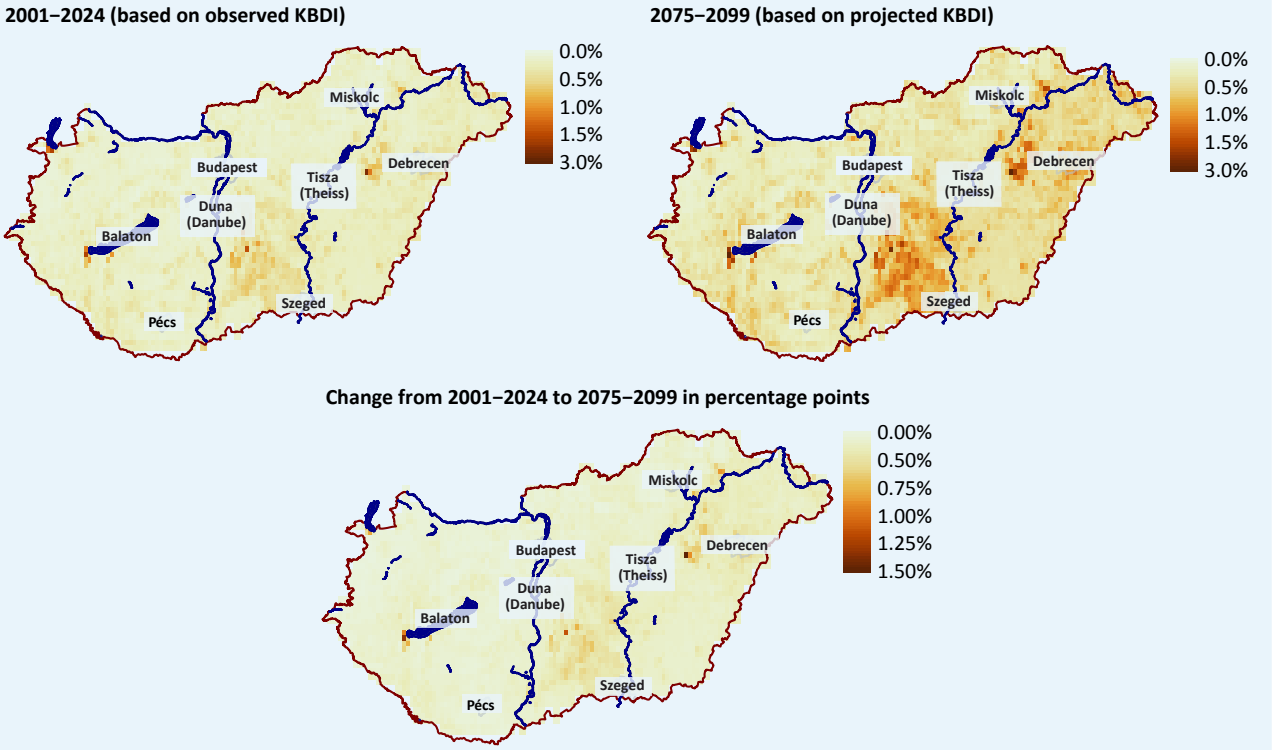

Table 7 summarises the implications of elevated fire risk for the banking sector, specifically the collateral-weighted projected monthly fire risk probabilities for Hungary under the RCP8.5 scenario, using June–September KBDI values. Grid-cell–level fire risk predictions were aggregated to postal code zones (i.e. the most detailed spatial information available for collaterals), and weighted by collateral values. Metrics are for: (i) mean value, (ii) the confidence interval of the mean, (iiI) the fire risk probabilities using the 95th percentile of the various climate models' KBDI values, and (iv) the confidence interval of the 95th percentile.

Results indicate that collateral-weighted fire occurrence risk is lower for both corporate and household exposures than the national unweighted average (compared with **Table 6**). Corporate collaterals appear slightly less exposed than household ones, although the difference is marginal. Nevertheless, average occurrence risks are projected to rise by roughly 88% (0.32% vs. 0.17%) for corporate collaterals, with the possibility of quadrupling (0.69% / 0.17%) in extreme years by the end of the century. If fire duration, intensity, and damage functions remain unchanged (an assumption that is far from certain), such increases would translate directly into proportionally higher fire-related damages. Results for households depict a similarly bleak picture.

Table 7
Collateral-value weighted fire occurrence risk in the RCP8.5 scenario, JJAS only. The same values are visualized in Appendix 4.

	Mean	CI of the mean (95%)	95th percentile of climatic model KBDI values	CI of the 95th percentile
Corporates, 2001-2024	0.17%	NA	NA	NA
Corporates, 2025-2049	0.21%	0.1-0.33%	0.48%	0.36-0.6%
Corporates, 2050-2074	0.23%	0.1-0.36%	0.56%	0.44-0.69%
Corporates, 2075-2099	0.32%	0.13-0.5%	0.69%	0.51-0.88%
Households, 2001-2024	0.19%	NA	NA	NA
Households, 2025-2049	0.23%	0.11-0.36%	0.52%	0.4-0.64%
Households, 2050-2074	0.25%	0.11-0.39%	0.62%	0.49-0.76%
Households, 2075-2099	0.35%	0.15-0.55%	0.76%	0.56-0.96%

6 Conclusion

The aim of this paper was to present a methodology to develop multi-decade predictions for fire occurrence risk, in order to aid long term decisions and to help in grasping the implications of climate change for financial institutions. Credit risk levels estimated by lenders should adequately reflect the worsening physical risk situations stemming from climate change, particularly in the case of loans with long maturities.

Most existing fire risk studies focus on immediate or near-term fire predictions. Decisions with long-term consequences, however, require models with a temporal focus of several decades, which necessarily carry high levels of uncertainty. Therefore, the use of robust statistical models and similarly long training data are required to lend credibility to the undertaking. At the same time, data on fire occurrences, particularly in Europe, have been strongly influenced by human involvement in setting fires. Without controlling for the Human Factor, models suffer from omitted variable bias, sometimes resulting in an apparent negative relationship between weather-based fire danger indices and fire risk.

In this paper, we used the Keetch-Byram Drought Index (KBDI) to explain fire occurrence risk in Hungary. In addition, we tested multiple candidates to express the Human Factor in the data, and arrived at the conclusion that a Google Trends-based, averaged, annualized time series of the terms 'climate', 'drought' and 'fire' contributes most to the model to capture the actual Human Factor, and describe fire occurrences best. Alternatives such as the atmospheric CO2-concentration, or the newspaper coverage of climate change (in Europe, not specific to Hungary), performed at acceptable levels. While the Google Trends dataset or its alternatives are by no means causes to human involvement in fire protection, they describe the impact of legal changes, law enforcement, public interest, engagement and fire protection well. In future simulations, however, we kept the Human Factor variable at its latest, observed value constant, given the limits of fire protection. A fire not lit cannot be prevented twice.

Future climate simulations using RCP8.5 and the statistical model presented in the paper describe an average doubling in fire risk (+98 percent by the last quarter of the century, compared to 2001-2024), with five times the fire risk in extreme years. Whereas our model does not reflect vegetation drying, given the absence of such past episodes, the actual threat of wildfires should be explored further.

7 References

Abdollahi, A. and Pradhan, B. (2023) Explainable artificial intelligence (XAI) for interpreting the contributing factors feed into the wildfire susceptibility prediction model. *Science of the Total Environment* 879 (2023) 163004. DOI: http://dx.doi.org/10.1016/j.scitotenv.2023.163004

Agarwala, M., et al. (2022) Unintended consequences of Indian groundwater preservation law on crop residue burning. *Economic Letters*, 214, 110446.

Alcasena, F. J., Salis, M., Ager, A. A., Castell, R., & Vega-García, C. (2017). Assessing Wildland Fire Risk Transmission to Communities in Northern Spain. *Forests*, *8*(2), 30. https://doi.org/10.3390/f8020030

Andrade, C., & Bugalho, L. (2023). Multi-Indices Diagnosis of the Conditions That Led to the Two 2017 Major Wildfires in Portugal. *Fire*, *6*(2), 56. https://doi.org/10.3390/fire6020056

Aoyagi, M., Appelgren, E., Ballantyne, A.G., Boykoff, M., Bruns, C., Chandler, P., Daly, M., Fernández-Reyes, R., Jiménez Gómez, I.J., Hawley, E., Hayakawa, Y., Hwang, K., Lee, K., Lyytimäki, J., McAllister, L., Mervaala, E., Mocatta, G., Nacu-Schmidt, A., Osborne-Gowey, J., Pearman, O., Petersen, L.K., Rawn, A., Riegert, K., Simonsen, A.H., and Ytterstad, A. (2025). World Newspaper Coverage of Climate Change or Global Warming, 2004-2025. Media and Climate Change Observatory Data Sets. Cooperative Institute for Research in Environmental Sciences, University of Colorado. doi.org/10.25810/4c3b-b819

Appelgren, E., Ballantyne, A.G., Boykoff, M., Chandler, P., Fernández-Reyes, R., Hawley, E., Jiménez Gómez, I., Lyytimäki, J., McAllister, L., Mervaala, E., Mocatta, G., Nacu-Schmidt, A., Osborne-Gowey, J., Pearman, O., Petersen, L.K., Rawn A., Riegert, K., Simonsen, A.H., and Ytterstad, A. (2025). European Newspaper Coverage of Climate Change or Global Warming, 2004-2025. Media and Climate Change Observatory Data Sets. Cooperative Institute for Research in Environmental Sciences. doi.org/10.25810/fx6e-r462

Barbaglia, L., Fatica, S. and Rho, C. (2023) Flooded credit markets: physical climate risk and small business lending, European Commission, 2023, JRC136274.

Bohlmann, S. and Laine, M. (2024) Statistical calibration of probabilistic medium-range Fire Weather Index forecasts in Europe. *Nat. Hazards Earth Syst. Sci*., 24, 4225–4235, https://doi.org/10.5194/nhess-24-4225-2024, 2024.

Burger, C and Herzberg, J and Nuvoli, T (2024) Climate Change Risk Indicators for Central Banking: Explainable AI in Fire Risk Estimations. Working paper. https://ssrn.com/abstract=4865384 or http://dx.doi.org/10.2139/ssrn.4865384

Carmel Y., Paz S., Jahashan F., Shoshany, M. (2009) Assessing fire risk using Monte Carlo simulations of fire spread. *Forest Ecology and Management* 257 (2009) 370–377

Carnicer, J., Alegria, A., Giannakopoulos, C. *et al.* (2022) Global warming is shifting the relationships between fire weather and realized fire-induced CO_2 emissions in Europe. *Sci Rep* **12**, 10365 (2022). https://doi.org/10.1038/s41598-022-14480-8

Cerasoli, S., Caldeira, M. C., Pereira, J. S., Caudullo, G., de Rigo, D. (2016) Eucalyptus globulus and other eucalypts in Europe: distribution, habitat, usage and threats. In: San-Miguel-Ayanz, J., de Rigo, D., Caudullo, G., Houston Durrant, T., Mauri, A. (Eds.), European Atlas of Forest Tree Species. Publ. Off. EU, Luxembourg, pp. e01b5bb+. https://w3id.org/mtv/FISE-Comm/v01/e01b5bb

CLC (2018) CORINE Land Cover, Copernicus Land Monitoring Service. Available at: https://land.copernicus.eu/en/products/corine-land-cover?tab=overview, accessed on the 14th April 2025. 04. 14.

Copernicus Emergency Management Service, 2019. **Fire danger indices historical data from the Copernicus Emergency Management Service**. In: *Copernicus Climate Change Service (C3S) Climate Data Stor*e (CDS). https://doi.org/10.24381/cds.0e89c522

Coskuner K. A. (2022). Assessing the performance of MODIS and VIIRS active fire products in the monitoring of wildfires: a case study in Turkey. *iForest* 15: 85-94. - doi: 10.3832/ifor3754-015

de Rigo, D., Libertà, G., Houston Durrant, T., Artés Vivancos, T., San-Miguel-Ayanz, J., 2017. **Forest fire danger extremes in Europe under climate change: variability and uncertainty**. *Publications Office of the European Union*, Luxembourg, 71 pp. ISBN: 978-92-79-77046-3 https://doi.org/10.2760/13180

Demirdogen, A. (2024) Stubble burning: What determines this fire? *Environmental Development*, Volume 51, 2024, 101029, https://doi.org/10.1016/j.envdev.2024.101029

Dijkstra, J., Durrant, T., San-Miguel-Ayanz, J., & Veraverbeke, S. (2022). Anthropogenic and Lightning Fire Incidence and Burned Area in Europe. *Land*, *11*(5), 651. https://doi.org/10.3390/land11050651

European Commission – DG ENTR (2012), EU-DEM Version 1, available from http:// http://epp.eurostat.ec.europa.eu/portal/page/portal/gisco_Geographical_information_maps/introduction and http://www.eea.europa.eu/data-and-maps/data/eu-dem.

Fontana A., Jarmulska B., Scheid, B., Scheins C., Schwarz C. (2025) From flood to fire: is physical climate risk taken into account in banks' residential mortgage rates? ECB Working Paper Series, No. 3036. Available at SSRN: https://ssrn.com/abstract=5176497 or http://dx.doi.org/10.2139/ssrn.5176497

Giglio, L., Schroeder W., Hall, J. V., Justice, O. C. (2018) MODIS Collection 6 Active Fire Product User's Guide, Revision B. NASA, available at: https://modis-fire.umd.edu/files/MODIS_C6_Fire_User_Guide_B.pdf

Herr, A., O'Connell, D., Dunlop, M., Unkovich, M., Poulton, P. and Poole, M. (2012), Second harvest–Is there sufficient stubble for biofuel production in Australia?. Glob. Change Biol. Bioenergy, 4: 654-660. https://doi.org/10.1111/j.1757-1707.2012.01165.x

INCF (2025) Registos individuais de incêndios 2001 a 2023. Available at: https://www.icnf.pt/florestas/gfr/gfrgestaoinformacao/estatisticas, accessed on the 9th April 2025.

Jacob, D., Petersen, J., Eggert, B., Alias, A., Christensen, O. B., Bouwer, L. M., Braun, A., Colette, A., Déqué, M., Georgievski, G., Georgopoulou, E., Gobiet, A., Menut, L., Nikulin, G., Haensler, A., Hempelmann, N., Jones, C., Keuler, K., Kovats, S., Kröner, N., Kotlarski, S., Kriegsmann, A., Martin, E., van Meijgaard, E., Moseley, C., Pfeifer, S., Preuschmann, S., Radermacher, C., Radtke, K., Rechid, D., Rounsevell, M., Teichmann, C., Tsikliras, A., Weber, B., Yiou, P. (2014). EURO-CORDEX: new high-resolution climate change projections for European impact research. Regional Environmental Change, 14(2): 563–578. https://doi.org/10.1007/s10113-013-0499-2

Jolly, W. Matt; Freeborn, Patrick H.; Bradshaw, Larry S.; Wallace, Jon; Brittain, Stuart. (2024). Modernizing the US National Fire Danger Rating System (version 4): Simplified fuel models and improved live and dead fuel moisture calculations. *Environmental Modelling and Software*. 181: 106181.

Keetch, J. J, and Byram G. M. (1968). A drought index for forest fire control. USDA Forest Service Research Paper, SE-38, 1-32.

Kotlarski, S., Keuler, K., Christensen, O.B., Colette, A., Déqué, M., Gobiet, A., & Wulfmeyer, V., 2014: Regional climate modeling on European scales: a joint standard evaluation of the EURO-CORDEX RCM ensemble. Geoscientific Model Developement, 7: 1297–1333, https://doi.org/10.5194/gmd-7-1297-2014

Laurent, P., Mouillot, F., Vanesa Moreno M., Yue C, and Ciais P. (2019) Varying relationships between fire radiative power and fire size at a global scale. *Biogeosciences*, 16, 275–288, 2019 https://doi.org/10.5194/bg-16-275-2019

Leone, V., Lovreglio, R., Martín, M.P., Martínez, J., Vilar, L. (2009). Human Factors of Fire Occurrence in the Mediterranean. In: Chuvieco, E. (eds) Earth Observation of Wildland Fires in Mediterranean Ecosystems. Springer, Berlin, Heidelberg. https://doi.org/10.1007/978-3-642-01754-4_11

Liu, T., et al. (2019) Missing emissions from post-monsoon agricultural fires in northwestern India: regional limitations of MODIS burned area and active fire products. *Environmental Research Communications*, (1)011007.

Martínez, J., Vega-Garcia, C., Chuvieco, E., (2009) Human-caused wildfire risk rating for prevention planning in Spain. *Journal of Environmental Management* 90, 1241–1252.URL: https://www.sciencedirect.com/science/article/pii/S0301479708001758, doi:10.1016/j.jenvman.2008.07.005.

Matthews, S. (2009) A comparison of fire danger rating systems for use in forests. *Australian Meteorological and Oceanographic Journal 58* (2009) 41-48

McArthur, A.G. (1967). "Fire behaviour in eucalypt forests. Forestry and Timber Bureau

McDowell, N. G., Allen, C. D. (2015) **Darcy's law predicts widespread forest mortality under climate warming**. *Nature Climate Change* 5 (7), 669-672. https://doi.org/10.1038/nclimate2641 , INRMM-MiD:13618830 (Cited 2 times on pages 1 and 11).

McNorton, J. R. and Di Giuseppe, F.: A global fuel characteristic model and dataset for wildfire prediction, Biogeosciences, 21, 279–300, https://doi.org/10.5194/bg-21-279-2024, 2024.

McNorton, J. R., Di Giuseppe, F., Pinnington, E., Chantry, M., & Barnard, C. (2024). A global probability-of-fire (PoF) forecast. *Geophysical Research Letters*, 51, e2023GL107929. **https://doi.org/10.1029/2023GL107929**

NASA VIIRS Land Science Team. (2021). *VIIRS (NOAA-21/JPSS-2) I Band 375 m Active Fire Product NRT (Vector data)* [Data set]. NASA LANCE MODIS at the MODAPS. https://doi.org/10.5067/FIRMS/MODIS/MCD14DL.NRT.0061

National Fire Danger Rating System (NFDRS) (2006) In Van Nostrand's Scientific Encyclopedia, G.D. Considine (Ed.). https://doi.org/10.1002/0471743984.vse8649

Pausas, J. G., Fernández-Muñoz, S. (2012) **Fire regime changes in the Western Mediterranean Basin: from fuel-limited to drought-driven fire regime**. *Climatic Change 110* (1-2), 215-226. https://doi.org/10.1007/s10584-011-0060-6 , INRMM-MiD:9112219

Prestemon, J. P., & Butry, D. T. (2010). Wildland arson: a research assessment. *In: Pye, John M.; Rauscher, H. Michael; Sands, Yasmeen; Lee, Danny C.; Beatty, Jerome S., tech. eds. Advances in threat assessment and their application to forest and rangeland management. Gen. Tech. Rep. PNW-GTR-802. Portland, OR: US Department of Agriculture, Forest Service, Pacific Northwest and Southern Research Stations: 271-283*, *802*, 271-283.

Szentimrey, T.: Manual of homogenization software MASHv3.03. Hungarian Meteorological Service, 71 pp. (2017)

Tinoco-Orozco D. A. , Vega-Nieva, D., Briseño-Reyes, J., Dominguez-Amaya, M., Adrián Israel Silva-Cardoza, Briones-Herrera, C., Ruiz-González, A. D. (2025). Where do fires burn more intensely? modeling and mapping maximum MODIS fire radiative power from aboveground biomass by fuel type in mexico. *Fire, 8*(2), 54. https://doi.org/10.3390/fire802005

van Vuuren D.P., Edmonds J., Thomson A., Riahi K., Kainuma M., Matsui T., … & Hibbard K.A., 2011: Representative concentration pathways: An overview. Climatic Change, 109: 5–31. https://doi.org/10.1007/s10584-011-0148-z

Van Wagner, C.E., and T.L. Pickett. (1985) *Equations and FORTRAN Program for the Canadian Forest Fire Weather Index System*. Ottawa: Canadian Forest Service.

Várgedő, B., Burger, C. and Kim D. (2025) Green Firms Are Less Risky: Results from a Preferential Capital Requirement Programme in Emerging Europe. MNB Working Papers, 2025/2, available at: https://www.mnb.hu/en/publications/studies-publications-statistics/working-papers-1-1/wp-2025-2-balint-vargedo-csaba-burger-donat-kim-green-firms-are-less-risky-results-from-a-preferential-capital-requirement-programme-in-emerging-europe

Wagner, van, C. E. (1987) Development and structure of the Canadian forest fire weather index system (Vol. 35), 1987.

Xu, C., You, C. (2023) Agricultural expansion dominates rapid increases in cropland fires in Asia, *Environment International*, Volume 179, 2023, 108189, https://doi.org/10.1016/j.envint.2023.108189.

Yıldırım, A. (2023). The Stubble Burning Problem in Sustainable Agriculture. International Journal of Innovative Engineering Applications, 7(1), 1-6. https://doi.org/10.46460/ijiea.1115461

8 Appendix

Appendix 1. The annualized value for the 'Human Factor' using data from Google Trends

Note: To arrive at the 'Annual value', the monthly values for 'climate', 'drought' and 'fire' were added up for each year, and were then summed. We took the 2-year moving average to account for the preceding year's impact in order to arrive at the Human Factor variable.

year	annual value	The Human Factor (2 yrs moving average)
2001	307 (backfilled)	307
2002	307 (backfilled)	307
2003	307 (backfilled)	307
2004	307	307
2005	540	423,5
2006	410	475
2007	436	423
2008	368	402
2009	407	387,5
2010	359	383
2011	451	405
2012	650	550,5
2013	548	599
2014	503	525,5
2015	628	565,5
2016	529	578,5
2017	615	572
2018	678	646,5
2019	816	747
2020	737	776,5
2021	727	732
2022	1117	922
2023	777	947
2024	1010	893,5

Appendix 2. Projected fire occurrence risk (The mean of all six climate model projections is shown in blue, complemented with the statistical uncertainty of the binomial regression of this paper, a 95 percent confidence interval, by the dashed lines. The 95th percentile of the climate model projections is shown in red, with the statistical 95 percent confidence interval depicted by the dashed lines. Fire occurrence risk of the past years, shown by the dot, is based on observed KBDI, the Human Factor value of 2024, and the binomial regression introduced by this paper.)

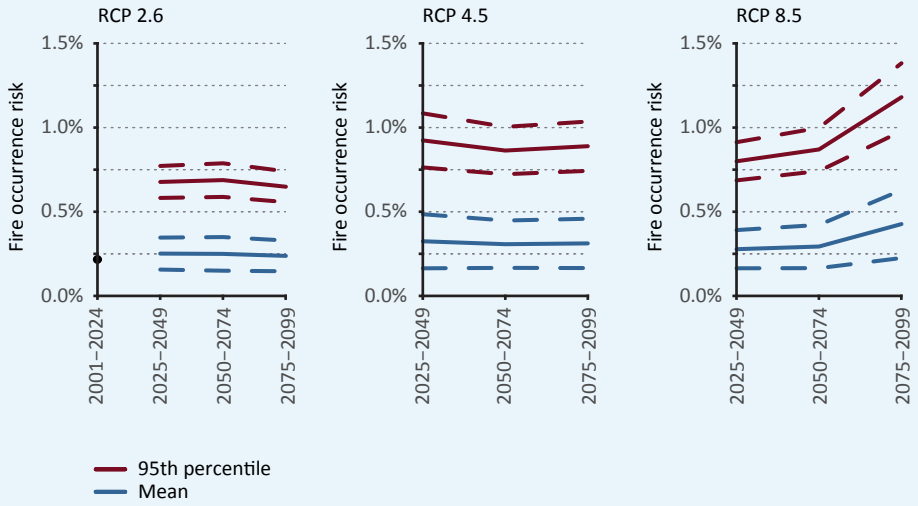

Appendix 3. Projected fire occurrence risk results by the GCM-RCM combinations used

Simulation	Mean	CI (95%)	95th percentile	CI (95%) of the 95th percentile
2025-2049 – RCP 2.6				
ICHEC-EC-EARTH_CLMcom-CCLM4-8-17	0.25%	0.16-0.34%	0.67%	0.58-0.76%
ICHEC-EC-EARTH_DMI-HIRHAM5_v2	0.23%	0.14-0.32%	0.64%	0.55-0.73%
CNRM-CERFACS-CNRM-CM5_CNRM-ALADIN63_v2	0.26%	0.16-0.36%	0.70%	0.6-0.8%
CNRM-CERFACS-CNRM-CM5_KNMI-RACMO22E_v2	0.25%	0.15-0.34%	0.65%	0.56-0.74%
NCC-NorESM1-M_SMHI-RCA4_v1	0.24%	0.15-0.33%	0.61%	0.53-0.7%
NCC-NorESM1-M_GERICS-REMO2015_v1	0.28%	0.17-0.39%	0.77%	0.67-0.88%
2025-2049 – RCP 4.5				
ICHEC-EC-EARTH_CLMcom-CCLM4-8-17	0.25%	0.16-0.35%	0.67%	0.58-0.76%
ICHEC-EC-EARTH_DMI-HIRHAM5_v2	0.58%	0.17-1%	2.23%	1.81-2.65%
CNRM-CERFACS-CNRM-CM5_CNRM-ALADIN63_v2	0.28%	0.17-0.4%	0.80%	0.69-0.92%
CNRM-CERFACS-CNRM-CM5_KNMI-RACMO22E_v2	0.30%	0.17-0.42%	0.89%	0.77-1.02%
NCC-NorESM1-M_SMHI-RCA4_v1	0.31%	0.18-0.44%	0.89%	0.76-1.02%
NCC-NorESM1-M_GERICS-REMO2015_v1	0.23%	0.14-0.31%	0.60%	0.52-0.68%
2025-2049 – RCP 8.5				
ICHEC-EC-EARTH_CLMcom-CCLM4-8-17	0.23%	0.13-0.33%	0.72%	0.62-0.82%
ICHEC-EC-EARTH_DMI-HIRHAM5_v2	0.25%	0.15-0.36%	0.70%	0.6-0.8%
CNRM-CERFACS-CNRM-CM5_CNRM-ALADIN63_v2	0.33%	0.19-0.47%	0.95%	0.81-1.1%
CNRM-CERFACS-CNRM-CM5_KNMI-RACMO22E_v2	0.28%	0.16-0.41%	0.89%	0.77-1.01%
NCC-NorESM1-M_SMHI-RCA4_v1	0.30%	0.18-0.41%	0.78%	0.67-0.89%
NCC-NorESM1-M_GERICS-REMO2015_v1	0.27%	0.17-0.38%	0.76%	0.66-0.87%

Simulation	Mean	CI (95%)	95th percentile	CI (95%) of the 95th percentile
2050-2074 – RCP 2.6				
ICHEC-EC-EARTH_CLMcom-CCLM4-8-17	0.28%	0.16-0.41%	0.87%	0.75-0.99%
ICHEC-EC-EARTH_DMI-HIRHAM5_v2	0.33%	0.18-0.47%	0.87%	0.72-1.01%
CNRM-CERFACS-CNRM-CM5_CNRM-ALADIN63_v2	0.28%	0.18-0.39%	0.71%	0.61-0.82%
CNRM-CERFACS-CNRM-CM5_KNMI-RACMO22E_v2	0.21%	0.13-0.29%	0.57%	0.49-0.65%
NCC-NorESM1-M_SMHI-RCA4_v1	0.19%	0.12-0.26%	0.51%	0.44-0.58%
NCC-NorESM1-M_GERICS-REMO2015_v1	0.20%	0.12-0.28%	0.57%	0.5-0.65%
2050-2074 – RCP 4.5				
ICHEC-EC-EARTH_CLMcom-CCLM4-8-17	0.28%	0.17-0.4%	0.81%	0.69-0.92%
ICHEC-EC-EARTH_DMI-HIRHAM5_v2	0.48%	0.17-0.79%	1.58%	1.27-1.89%
CNRM-CERFACS-CNRM-CM5_CNRM-ALADIN63_v2	0.38%	0.22-0.55%	1.06%	0.89-1.22%
CNRM-CERFACS-CNRM-CM5_KNMI-RACMO22E_v2	0.22%	0.14-0.31%	0.62%	0.53-0.7%
NCC-NorESM1-M_SMHI-RCA4_v1	0.23%	0.15-0.32%	0.60%	0.51-0.68%
NCC-NorESM1-M_GERICS-REMO2015_v1	0.24%	0.15-0.32%	0.61%	0.52-0.7%
2050-2074 – RCP 8.5				
ICHEC-EC-EARTH_CLMcom-CCLM4-8-17	0.24%	0.15-0.33%	0.65%	0.56-0.74%
ICHEC-EC-EARTH_DMI-HIRHAM5_v2	0.28%	0.16-0.4%	0.83%	0.71-0.96%
CNRM-CERFACS-CNRM-CM5_CNRM-ALADIN63_v2	0.46%	0.22-0.7%	1.43%	1.19-1.67%
CNRM-CERFACS-CNRM-CM5_KNMI-RACMO22E_v2	0.29%	0.15-0.42%	0.92%	0.78-1.05%
NCC-NorESM1-M_SMHI-RCA4_v1	0.26%	0.16-0.35%	0.70%	0.6-0.79%
NCC-NorESM1-M_GERICS-REMO2015_v1	0.23%	0.15-0.32%	0.62%	0.53-0.71%
2075-2099 – RCP 2.6				
ICHEC-EC-EARTH_CLMcom-CCLM4-8-17	0.23%	0.14-0.31%	0.60%	0.52-0.69%
ICHEC-EC-EARTH_DMI-HIRHAM5_v2	0.23%	0.14-0.31%	0.58%	0.5-0.66%
CNRM-CERFACS-CNRM-CM5_CNRM-ALADIN63_v2	0.25%	0.15-0.34%	0.66%	0.57-0.76%
CNRM-CERFACS-CNRM-CM5_KNMI-RACMO22E_v2	0.30%	0.17-0.42%	0.89%	0.77-1.02%
NCC-NorESM1-M_SMHI-RCA4_v1	0.21%	0.13-0.28%	0.53%	0.46-0.6%
NCC-NorESM1-M_GERICS-REMO2015_v1	0.22%	0.14-0.31%	0.62%	0.54-0.71%
2075-2099 – RCP 4.5				
ICHEC-EC-EARTH_CLMcom-CCLM4-8-17	0.30%	0.16-0.45%	1.03%	0.88-1.17%
ICHEC-EC-EARTH_DMI-HIRHAM5_v2	0.36%	0.14-0.59%	0.95%	0.73-1.18%
CNRM-CERFACS-CNRM-CM5_CNRM-ALADIN63_v2	0.40%	0.21-0.6%	1.21%	1.02-1.41%
CNRM-CERFACS-CNRM-CM5_KNMI-RACMO22E_v2	0.24%	0.14-0.33%	0.70%	0.6-0.8%
NCC-NorESM1-M_SMHI-RCA4_v1	0.30%	0.18-0.42%	0.80%	0.68-0.91%
NCC-NorESM1-M_GERICS-REMO2015_v1	0.27%	0.17-0.36%	0.68%	0.59-0.78%
2075-2099 – RCP 8.5				
ICHEC-EC-EARTH_CLMcom-CCLM4-8-17	0.33%	0.19-0.46%	0.90%	0.77-1.04%
ICHEC-EC-EARTH_DMI-HIRHAM5_v2	0.50%	0.23-0.76%	1.52%	1.26-1.79%
CNRM-CERFACS-CNRM-CM5_CNRM-ALADIN63_v2	0.63%	0.27-0.99%	1.79%	1.43-2.15%
CNRM-CERFACS-CNRM-CM5_KNMI-RACMO22E_v2	0.38%	0.21-0.54%	1.05%	0.89-1.22%
NCC-NorESM1-M_SMHI-RCA4_v1	0.43%	0.25-0.61%	1.06%	0.88-1.24%
KBDI_NCC-NorESM1-M_GERICS-REMO2015_v1	0.31%	0.2-0.41%	0.70%	0.6-0.81%

Appendix 4. Projected fire occurrence risk, weighted by collateral value and postal code-level location as of 31st December 2024 in Hungary, JJAS only. (The mean of all six climate model projections is shown in blue, complemented with the statistical uncertainty of the binomial regression of this paper, a 95 percent confidence interval, by the dashed lines. The 95th percentile of the climate model projections is shown in red, with the statistical 95 percent confidence interval depicted by the dashed lines. Fire occurrence risk of the past years, shown by the dot, is based on observed KBDI, the Human Factor value of 2024, and the binomial regression introduced by this paper.)

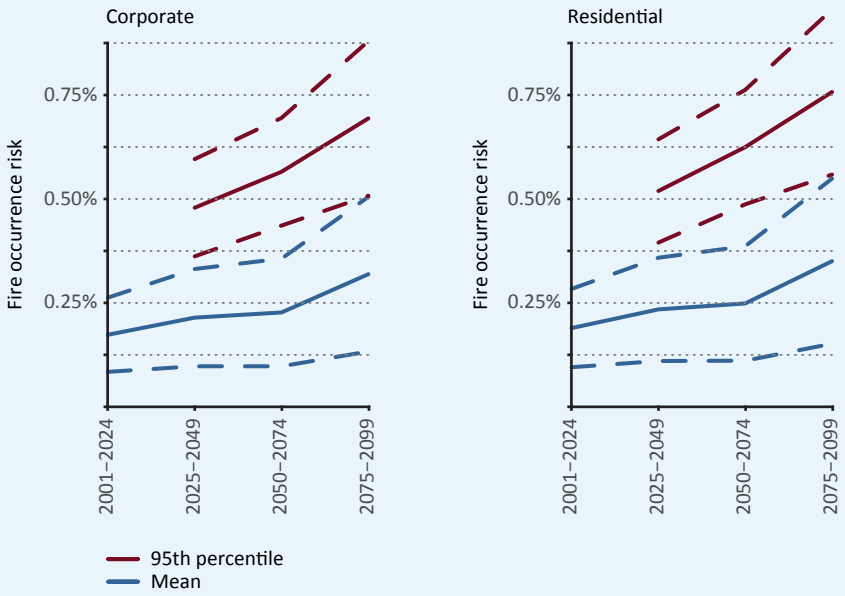

MNB WORKING PAPERS 2

THE HUMAN FACTOR IN WILDFIRES: TOWARDS A LONG-TERM FIRE RISK ESTIMATION MODEL FOR CENTRAL BANKING

June 2026

Print: Prospektus Kft.

6 Tartu u., Veszprém H-8200

mnb.hu

1054 BUDAPEST, SZABADSÁG TÉR 8–9.